Effects of Tube Wall Thickness on Combustion and Growth Rate of Supersonic Reacting Mixing Layer

Di Lu and Fang Chen

Abstract The study of supersonic reacting shear layer has been paid great attention to further understand flow characteristics and mechanism of the engine combustion process. However, most past studies remain narrow in focus dealing only with infinitely small tube thickness or fixed ones which neglects the complex flow structures reflecting some general features of scramjet engine mixing and combustion process. In the present study, supersonic reacting mixing layer has been studied under different tube thickness. Numerical simulations have been carried out with CFD++ 14.1 to solve the Reynolds averaged equation on the Evan's configuration which is closed by Menter's Shear Stress Transport turbulence model and finite reaction rate chemical kinetic model. The flow field evolution, mixing layer growth and combustion ignition are the major focus of current study. The obtained results show that the existence of finite tube thickness brings unique flow field characteristic such as expansion fans and shock systems which is not included in the tradition simplified analysis of reacting shear with infinitesimal tube thickness. The tube thickness has a positive effect on growth of mixing layer and ignition delay that 50% of decrease in ignition delay has achieved by enough tube wall thickness.

Keywords Supersonic reacting shear layer · Non-premixed turbulent combustion · Tube thickness effect

1 Introduction

In recent years, researchers have shown an increased interest in ramjet engine as propulsion system for hypersonic vehicles and orbit missions [1] for its low payload costs and high specific impulse [2]. However, effective operation of ramjet

D. Lu · F. Chen (✉)
Shanghai Jiao Tong University, Shanghai, China
e-mail: fangchen@sjtu.edu.cn

D. Lu
e-mail: ludi96@sjtu.edu.cn

engine over wide speed range is still tricky in the design of hypersonic vehicles [3]. One of the main obstacles is ignition and combustion stability in high speed flow [4] which requires fundamental study in supersonic combustion process. For this reason, the study of supersonic reacting shear layer aims to further understand flow characteristics and mechanism of the engine combustion process.

Since Zeldovich number [5] was proposed to describe the influence of free shear and flow Mach number on ignition, many researches have been conducted on ignition and flameout. It was found that shock wave impingement [6], vortex shedding [7], inflow fluctuation [8] and additive effects [9] acted a prominent role in ignition characteristic, whereas low temperature of mixture dominates rich combustion flameout [7]. In addition to combustion characteristics, compressibility has a negative effect on the growth rate of reacting shear layer [10], while heat release effect is closely related to the convective Mach number [11, 12]. The further reason of heat release and compressibility effect has been attributed to reduced production of Reynolds stress [13].

However, most previous studies are limited to the infinitesimal or fixed wall thickness, and only a few works consider the influence of the tube wall thickness [14, 15]. The effect of tube wall thickness on evolution of mixing layer and flow structure in supersonic reacting layer has not be systematically explored.

The aim of this investigation has been to establish relationship between tube wall thickness on flow filed characteristic of co-axial hydrogen and air jet flame. The paper is divided into 4 sections. The first section includes a review of the past studies on reacting mixing layer. The second section briefly introduces the numerical methods of the study and gives out model validation. The third section presents the simulation results under different tube thickness. The final section gives out the conclusion.

2 Numerical Methodology

2.1 Computational Fluid Dynamic

The Reynolds Average conservation equations of mass, momentum, species and energy for multicomponent compressible reacting system are solved by CFD++ 14.1 based on finite volume method. Multi-component diffusion model described by Fick's law has been applied for species transport property. The turbulence closure has been achieved by Menter's Shear Stress Transport (SST) model.

A nine-species, eighteen-step mechanism [16] is employed for the chemical kinetics of hydrogen and air. This model was validated in the CFD++ 11.1 official tutorial of Burrow combustor against experiment data. Nitrogen is defined as an inert gas which is evaluated automatically after other species are given.

The governing equations are solved by the finite-volume method approach. Second order differential scheme has been applied for inviscid term. Multi-dimensional total

variation diminishing (TVD) polynomial interpolation has been used for reconstructions over nodes. To accelerate the computation, a spatial discretization blending between first and second order has also been applied.

2.2 Model Validation

The baseline model used in this study is a confined coaxial hydrogen jet flame with a design Mach number of 2.0 [17] whose salient features are shown in Fig. 1. The radius of the internal hydrogen jet nozzle r_j is 3.2625 mm with a tube thickness δ_w of 1.5 mm, and the radius of the whole tube R is 32.65 mm. Since little knowledge of the nozzle lip structure was given, a straight wall is assumed to consider the boundary layer effect of the injector.

The inflow condition of the hydrogen jet is characterized by 251 K, 0.1 atm and 2.0 Ma with pure hydrogen. The inflow condition of the vitiated air is characterized by 1495 K, 0.1 atm and 1.9 Ma with species composed of 0.241 oxygen, 0.281 water, and 0.478 nitrogen. X-axial symmetry has been applied on the centerline of the tube to utilize the symmetry feature of the problem. No-slip adiabatic condition has been specified for the solid wall.

To establish the fidelity of the numerical simulation, grid convergence study has been conducted on the baseline geometry with three sets of computational meshes. These three sets of meshes are namely Mesh A, Mesh B and Mesh C containing 150, 250 and 490 K grid points respectively. The species distributions at different cross sections of the duct are in comparison with the experiment [17]. Figure 2 has given out the radial distribution of OH, H2O, N2, H2 at x/dj = 8.26, 15.5, 21.7 and 27.9. It is shown that the results for the Mesh B and Mesh C collapse almost perfectly, thus the further analysis is based on Mesh B. Some deviations have behaved between simulated results and experimental results for ignition delay. This is mainly caused by uncertainties in inflow turbulence boundary layer of the experiment configuration and deficiency of inconsideration of turbulence chemistry interaction in combustion process.
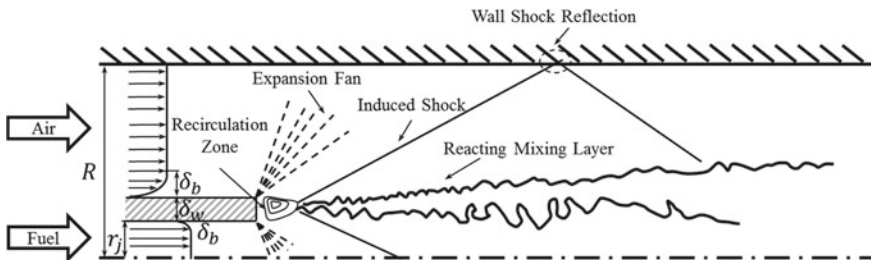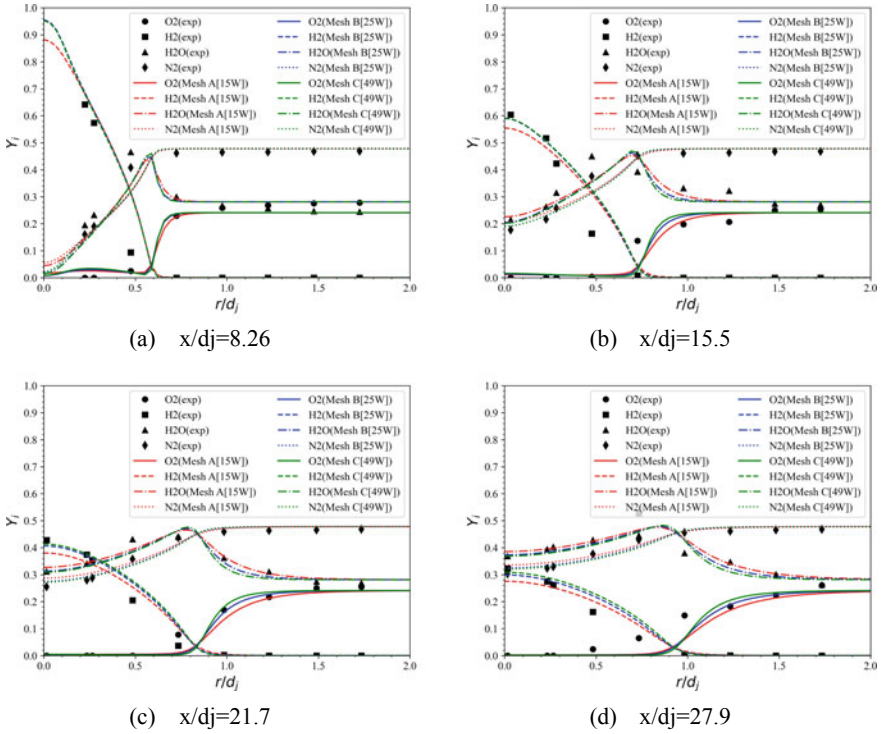

Fig. 1 Baseline configuration

Fig. 2 Comparison of species radial distribution at different cross section for x/dj = 8.26, 15.5, 21.7, 27.9

3　Result and Discussion

3.1　Flow Field Characteristic

In this section the general flow field characteristic has been analyzed under finite tube wall thickness and infinitesimal tube wall thickness. For the finite tube wall thickness case, a tube wall thickness of 1.5 mm has been applied just as the baseline model which has been discussed in Sect. 2.2. For the infinitesimal tube wall thickness condition, an inlet velocity profile has been applied characterized by the formula (1) below:

$$U = \frac{u_{up}+u_{down}}{2} + \frac{u_{up}-u_{down}}{2}\tanh\left(\frac{y-y_c}{2\delta_0}\right) \tag{1}$$

In which u_{up} and u_{down} are the velocity of air and fuel, y_c is the separation location of two fluid, δ_0 is considered as the initial mixing thickness.

From Fig. 3, a major difference of the flow fields between reacting mixing layer with and without tube wall thickness can be summarized to the existence of expansion
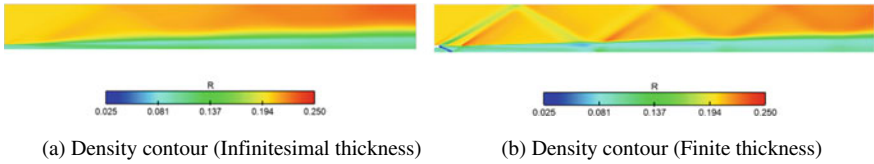
(a) Density contour (Infinitesimal thickness) (b) Density contour (Finite thickness)

Fig. 3 Density contour with and without finite tube wall thickness

waves, recirculation zone and reattached shocks which brings great complexity to the evolution of the flow field.

To better visualize the flow field with finite tube wall thickness, a contour graph of density gradient norm in global view is given in Fig. 4 to discriminate the shock structure combined with local streamlines. In Fig. 4a's global view, the flow field of supersonic reacting mixing layer with finite tube wall thickness is characterized by near-field expansion fan, shock wave, and recirculation zone combined with far-field shock reflection, shock-reacting layer interaction. From Fig. 4b, oxidant and fuel separated by finite tube thickness induces a recirculation zone downstream of the tube tip in the near-field. The inward wall causes two expansion fans surrounding the tube tip making the stream merge together. After the merge of the two streams, reattach shocks are formed reflecting outward leading to complex shock system in the tube. In the far-field, reattach shocks induced by merge of the stream turning outward strikes the outer tube wall and reflects inward impinging on the reacting mixing layer which leads to a strong local interaction with the reacting mixing layer. On the other hand, reattach shocks turning inward interacts with the one caused by the symmetry part, reflects outward and finally merges the reattach shocks turning outward after interaction with mixing layer.

Combustion process is another important flow field characteristic in reacting mixing layer which is given in Fig. 5. From Fig. 5a, the combustion process is started by ignition in mixing layer which characterized by premix combustion, then the flame extends to the core flow. The combustion mode in the core flow undergoes transition from non-premix to partially premix. From Fig. 5b, a clearer view of the
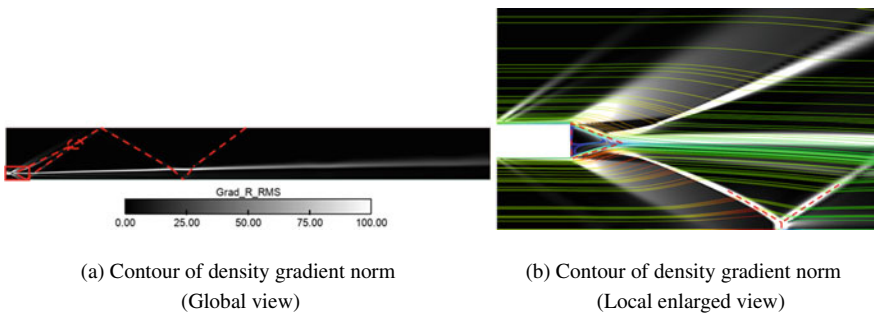

(a) Contour of density gradient norm (Global view) (b) Contour of density gradient norm (Local enlarged view)

Fig. 4 Contour of density gradient norm under finite tube wall thickness ($\delta_w = 1.5$ mm)

(a) Contour of flame index (FI)   (b) Velocity contour with OH and HO2
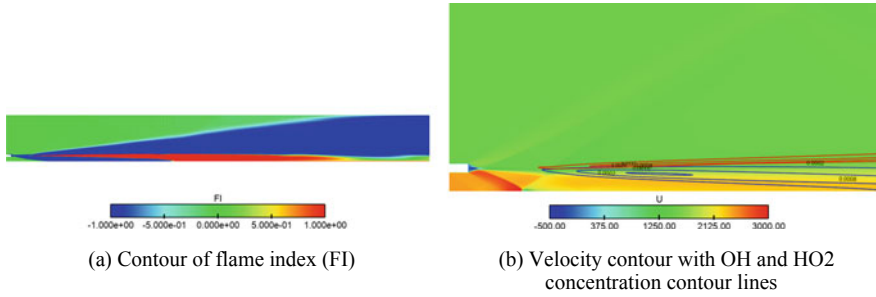   concentration contour lines

Fig. 5 Contour of flame index and velocity under finite tube wall thickness ($\delta_w = 1.5$ mm)

combustion process can be visualized by the OH (colored by red) and HO_2 (colored by blue) contour. On the outside edge of mixing layer, the OH species is majorly produced due to the fully mixing of fuel and oxygen. In the centerline region, high fuel concentration is exhibited which causes weak reaction leading to a region of fuel-rich combustion. As a result, the HO2 is majorly produced in the centerline region.

3.2 Effects of Tube Wall Thickness on Flow and Combustion

To study the effects of tube wall thickness, tube wall thicknesses of 0.5 mm, 0.8 mm, 1.0 mm, 1.5 mm, 2.5 mm have been applied other than the baseline case of 1.5 mm. The inflow mass flow rate is maintained during the variation of tube wall thickness.

First, flow field evolution under different tube wall thickness has been compared in Fig. 6. It shows that with the increase of the tube thickness a larger recirculation zone is formed which causes an enlarged initial expansion fan and weaker initial shock wave characterized by smaller shock angle. On the other hand, the bigger tube thickness leads to stronger overexpansion in the inner fuel inject and thus finally
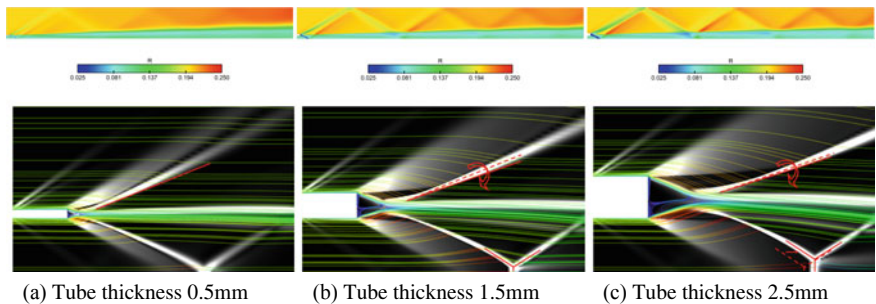

(a) Tube thickness 0.5mm   (b) Tube thickness 1.5mm   (c) Tube thickness 2.5mm

Fig. 6 Comparison of flow structure at different tube thickness for t = 0.5 mm, 1.5 mm, 2.5 mm

results in Mach disk in the center of the jet flow. The location of Mach disk can be estimated by an empirical expression as proportional to square root of ratio between nozzle total pressure and back pressure (Ashkenas and Sherman 1966) as formula (2) which agrees well with the simulation results. With the increase of tube wall thickness from 0.5 mm to 2.5 mm, the Mach disk position has been postponed by 16%.

$$\frac{x_M}{d} \propto \sqrt{\frac{P_{tot}}{P_b}} \tag{2}$$

Figure 7 gives out the growth of the reacting layer characterized by the vorticity thickness which is defined in formula (3):

$$\theta_w = \frac{\Delta U}{\left(\frac{\partial U}{\partial y}\right)_{max}} = \frac{u_{up} - u_{down}}{\left(\frac{\partial U}{\partial y}\right)_{max}} \tag{3}$$

Figure 7 indicates a general trend that increase of the tube wall thickness leads to larger reacting mixing layer growth, which can be also seen clearly from the vorticity contour from Fig. 8. The major reason attributes to a more vortex generation due to the larger tube wall thickness. On the other hand, sudden drops can be visualized in the stream wise distribution of vorticity thickness which is always co-occurrence of shock impinge indicated by stream wise Mach number monitor. Such a fact indicates that the shock wave impinge has a strong depression effect on the growth rate of mixing reacting layer which is attributed to the great compression effect brought by the shock wave. Downstream of the shock, the growth rate of the mixing reacting
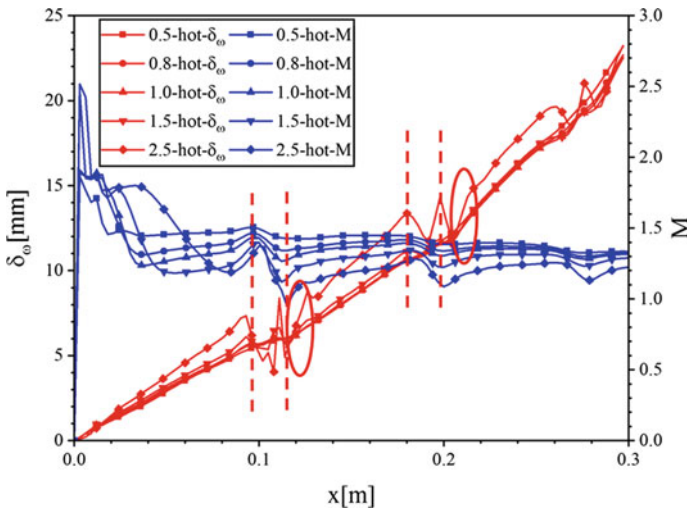

Fig. 7 Streamwise vorticity thickness distribution and Mach number distribution at different tube thickness for t = 0.5 mm, 0.8 mm, 1.0 mm, 1.5 mm, 2.5 mm
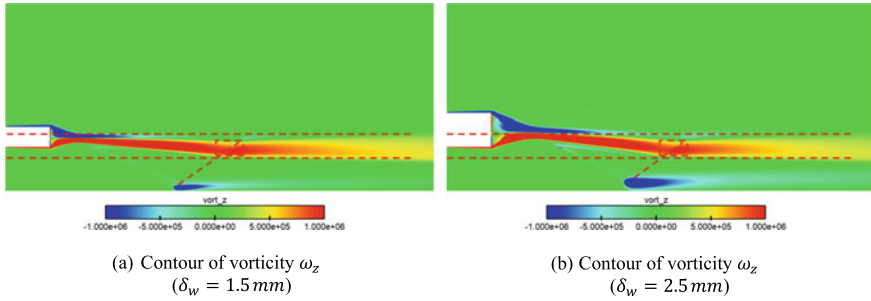
(a) Contour of vorticity ω_z
($\delta_w = 1.5\,mm$)

(b) Contour of vorticity ω_z
($\delta_w = 2.5\,mm$)

Fig. 8 Vorticity contour under tube wall thickness of 1.5 mm, 2.5 mm

layer faces a rapid increase due to the increase of the vorticity magnitude which can be observed from Fig. 8.

To express the effect of wall thickness on combustion process, species indicator combined with the combustion efficiency have been used to represent the microscopic and macroscopic view point of combustion. The species indicator is defined as the maximum concentration in a section, while consumption of the fuel is utilized to evaluate the combustion efficiency.

From Fig. 9a, with the increase of tube thickness, combustion happens with less ignition delay. In detail, at a smaller tube thickness of 0.5 mm and 0.8 mm, the ignition happens almost the same position for not enough large recirculation zone to support early mixing. With an enough large recirculation zone formed by large tube thickness, the ignition delay is decreased by 50% relative to the low tube wall thickness. However, even larger tube thickness makes no contribution to less ignition delay. In current case, the threshold value of tube thickness is 1.5 mm. One more interesting founding can be observed from Fig. 9b that though increase of tube thickness leads to early combustion it does not necessarily increase the total combustion efficiency.
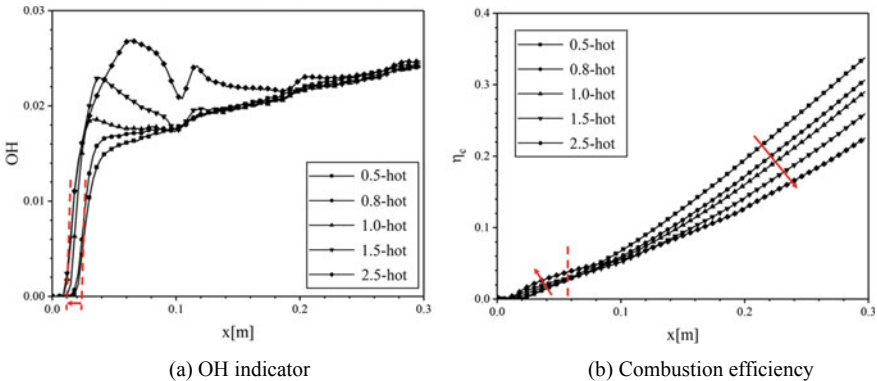

(a) OH indicator

(b) Combustion efficiency

Fig. 9 Comparison of combustion process at different tube thickness

4 Conclusion

The effects of tube thickness on supersonic reacting mixing layer growth and combustion process have been investigated in this paper, the conclusions are as follow:

(1) Tube thickness has significant impact on the growth of reacting mixing layer and combustion process for the introduction of complex shock systems.
(2) The increase of tube thickness increases the mixing layer thickness growth which promotes more thorough mixing. On the other hand, the ignition delay is 50% less than that of the infinite tube when the tube wall thickness is 1.5 mm. However, there is a thickness threshold for the above effects that the increase of thickness above the threshold will not further reduce the ignition delay. Under the current situation, the threshold value of tube thickness is 1.5 mm.

References

1. Fry RS (2004) A century of ramjet propulsion technology evolution. J Propul Power 20:27–58. https://doi.org/10.2514/1.9178
2. Huang W, Yan Li, Tan J-G (2014) Survey on the mode transition technique in combined cycle propulsion systems. Aerosp Sci Technol 39:685–691. https://doi.org/10.1016/j.ast.2014.07.006
3. Firsov A, Savelkin KV, Yarantsev DA (2015) Plasma-enhanced mixing and flameholding in supersonic flow. Phil Trans Royal Soc A: Math, Phys Eng Sci 373(2048):20140337. https://doi.org/10.1098/rsta.2014.0337
4. Capecelatro J, Bodony DJ, Freund JB (2019) Adjoint-based sensitivity and ignition threshold mapping in a turbulent mixing layer. Combust Theor Model 23(1):147–179. https://doi.org/10.1080/13647830.2018.1495342
5. Jackson TL, Hussaini MY (1988) An asymptotic analysis of supersonic reacting mixing layers. Combust Sci Technol 57(4–6):129–140
6. Huete C, Sánchez AL, Williams FA (2017) Diffusion-flame ignition by shock-wave impingement on a hydrogen–air supersonic mixing layer. J Propul Power. 256-263. https://doi.org/10.2514/1.B36236
7. Zhang YL, Wang B, Zhang HQ (2014) Ignition, flame propagation and extinction in the supersonic mixing layer flow. Sci China Technol Sci 57(11):2256–2264. https://doi.org/10.1007/s11431-014-5655-5
8. Tahsini AM (2013) Turbulence and additive effects on ignition delay in supersonic combustion. Proc Inst Mech Eng, Part G: J Aerosp Eng 227(1):93–99. https://doi.org/10.1177/0954410011428981
9. Tien JH, Stalker RJ (2002) Release of chemical energy by combustion in a supersonic mixing layer of hydrogen and air. Combust Flame 131(3):329–348. https://doi.org/10.1016/s0010-2180(02)00371-1
10. Givi P, Madnia CK, Steinberger CJ et al (1991) Effects of compressibility and heat release in a high speed reacting mixing layer. Combust Sci Technol 78(1–3):33–67. https://doi.org/10.1080/00102209108951740

11. Calhoon W (2003) Heat release and compressibility effects on planar shear layer development. 41st Aerospace sciences meeting and exhibit. 1273. https://doi.org/10.2514/6.2003-1273
12. Yao X, Tan J, Zhang D (2019) Combustion of H2/air supersonic mixing layers with splitter plate: Growth rates and transport characteristic. Acta Astronaut 165:401–413. https://doi.org/10.1016/j.actaastro.2019.09.036
13. Liu H, Gao Z, Jiang C et al (2019) Numerical study of combustion effects on the development of supersonic turbulent mixing layer flows with WENO schemes. Comput Fluids 189:82–93. https://doi.org/10.1016/j.compfluid.2019.05.019
14. Otakeyama Y, Takeshi Yokomori T, Mizomoto M (2009) Stability of CH4—N2/Air jet diffusion fame for various burner rim thicknesses. Proc Combust Inst 32:1091–1097. https://doi.org/10.1016/j.proci.2008.05.002
15. Zhang L, Choi JY, Yang V (2015) Supersonic combustion and flame stabilization of coflow ethylene and air with splitter plate. J Propul Power 2015:1–14. https://doi.org/10.2514/1.B35740
16. Drummond JP, Rogers RC, Hussaini MY (1987) A numerical model for supersonic reacting mixing layers. Comput Methods Appl Mech Eng 64:39–60. https://doi.org/10.1016/0045-7825(87)90032-6
17. Evans JS, Schexnayder Jr CJ, Beach Jr HL (1978) Application of a two-dimensional parabolic computer program to prediction of turbulent reacting flows. https://ntrs.nasa.gov/archive/nasa/casi.ntrs.nasa.gov/19780012520.pdf